


# An Analytical Effective-Diode-Based Analysis of Industrial Solar Cells From Three-Diode Lumped-Parameter Model

Chuanzhong Xu, Xiaofang Sun, Ying Liang, Gongyi Huang, and Fei Yu 

**Abstract**—Three-diode lumped-parameter equivalent circuit model conforms to photovoltaic device physics and processes an exact analysis for  $I$ - $V$  characteristics of industrial solar cells, because it explains the different leakage current components especially for recombination current resulting from defects or grain boundaries. However, three-diode model's complete circuit topology leads to complicated transcendental  $I$ - $V$  equation without analytical solution so that low computation efficiency limits three-diode model's applications in photoelectric simulations. In this article, an effective-diode method is proposed to simplify three-diode model, derive accurate and efficient terminal current-voltage solution to three-diode model, and acquire electrostatic characteristics of the solar cells. The calculated values have good agreements with numerical iteration results and experimental data measured from solar cells, respectively. Finally, the effective-diode method performs an important role of solving three-diode model analytically, predicting  $I$ - $V$  characteristics of industrial solar cells accurately, and providing three-diode model's practicability and development in solar cells' simulations.

**Index Terms**—Effective-diode method, equivalent circuit, solar cells, three-diode lumped-parameter model.

## I. INTRODUCTION

SERVING as a clean and gentle energy source to the earth, solar cells have been increasingly used into practical applications. Recently, designing and applying solar cells into photovoltaic circuits and systems are still the research hot spots in both academic and industrial areas. As the most common approach to analyze the electrostatic characteristics of solar cells, an accurate and efficient lumped-parameter equivalent circuit model is very important and urgently necessary.

According to the difference in circuit topology's complexity, one-, two-, and three-diode lumped-parameter equivalent circuit models [1]–[8] are shown in Fig. 1. One-diode model [1]–[3] in Fig. 1(a) processes the simplest circuit topology and the lowest computation complexity. One-diode

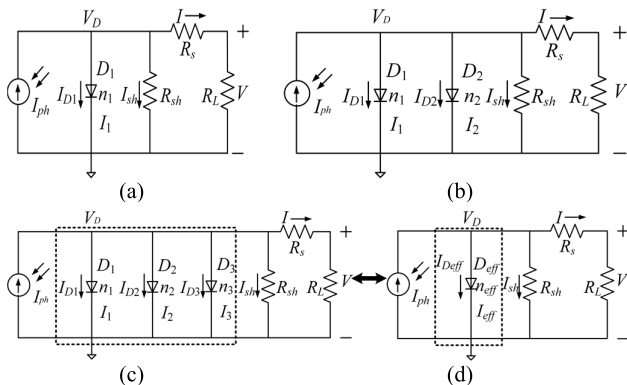


Fig. 1. Lumped-parameter equivalent circuit models of solar cells. (a) One-diode model. (b) Two-diode model. (c) Three-diode model. (d) Effective one-diode model transformed from three-diode model.

models [1]–[3] are primarily based on the combination of a light generated current source  $I_{ph}$  and single one diode  $D_1$  representing the diffusion and recombination current in the quasi-neutral regions of the emitter and bulk regions. Thus, it has a good balance between accuracy and efficiency, which makes it possible to be implemented into simulators. In addition,  $I_s$  resulting from the shunt resistance  $R_{sh}$  represents the leakage current across the p-n junction, the series resistance  $R_s$  represents contact resistance and resistance in the emitter and bulk regions, and  $R_L$  is the load resistance. As shown in Fig. 1(b) and (c), multiple-diode models [4]–[8] including two- [4], [5] and three-diode [6]–[8] models are proposed to increase the accuracy of simulation by adding diode  $D_2$  and  $D_3$  in parallel with  $I_{ph}$ , where  $D_2$  is added to represent the current component due to recombination in the space charge regions, and  $D_3$  is used to consider the contribution of recombination current resulting from defects and grain sites in solar cells. Unfortunately, multiple-diode models have not obtained the extensive applications. One of the main challenges for implementing multiple-diode models is how to solve  $I$ - $V$  equation and maximum power point analytically, as these models have a transcend  $I$ - $V$  equation including at least two exponent items. In fact, a tradeoff between the accuracy and efficiency is a key feature to implement lumped-parameter models into photovoltaic device, circuit, and system simulators. From the accuracy aspect, multiple-diode models give better simulations for industrial solar cells. However, from the efficiency aspect, the more complicated circuit topologies of multiple-diode models lead to much more complicated transcend  $I$ - $V$  equation, which is accompanied by

Manuscript received January 12, 2021; revised February 25, 2021; accepted March 30, 2021. Date of publication April 14, 2021; date of current version May 21, 2021. This work was supported in part by the National Natural Science Foundation of China under Grant 61904056 and in part by the Fundamental Research Funds for the Central Universities under Grant ZQN-809. The review of this article was arranged by Editor B. Hoex. (Corresponding author: Fei Yu.)

The authors are with the College of Information Science and Engineering, Huaqiao University, Xiamen 361021, China (e-mail: yufei\_jnu@126.com).

Color versions of one or more figures in this article are available at <https://doi.org/10.1109/TED.2021.3070839>.

Digital Object Identifier 10.1109/TED.2021.3070839

low calculation efficiency because analytical solution has not been derived, until now. Obviously, the absence of analytical solution is the bottleneck blocking that the multiple-diode model comes into practical applications. Therefore, analytical solution to solar cells' multiple-diode model, especially for three-diode model, is urgently necessary to facilitate researchers to comprehend the electrostatic characteristics [9], [10], complete photovoltaic device simulations [11]–[14] and parameter-extractions [15]–[19], and optimize the preparation processes [20], [21].

In this article, we focus on deriving the analytical solution to the three-diode lumped-parameter model of industrial solar cells. First, we proposed the effective-diode method to simplify the complicated three-diode circuit topology into effective one-diode circuit topology, as shown in Fig. 1(d). Second, based on the effective-diode method, we derive the analytical solution to the three-diode model to acquire the  $I$ - $V$  and  $P$ - $V$  curves of solar cells. Third, we determine the four key feature parameters of solar cells, i.e., short-circuit current  $I_{sc}$ , open-circuit voltage  $V_{oc}$ , the maximum power point ( $V_m$ ,  $P_m$ ), and fill factor (FF). Finally, we use numerical iteration results and experimental data of the different industrial PV modules to validate our proposed analytical solution. As a result, good agreements show that the effective-diode-based analytical solution could be used to implement three-diode lumped-parameter model into simulations of industrial solar cells.

## II. EFFECTIVE-DIODE METHOD

From the three-diode model of solar cells shown in Fig. 1(c), we can use Kirchhoff's current law and standard diode equation [22] to derive the terminal  $I$ - $V$  equation as

$$I = I_{ph} - I_1 \left( e^{\frac{V_D}{n_1 V_t}} - 1 \right) - I_2 \left( e^{\frac{V_D}{n_2 V_t}} - 1 \right) - I_3 \left( e^{\frac{V_D}{n_3 V_t}} - 1 \right) - \frac{V_D}{R_{sh}}. \quad (1)$$

Here  $n_1$ ,  $n_2$ , and  $n_3$  are the ideality factors of three diodes representing the divergence from the ideal diode, respectively.  $I_1$ ,  $I_2$ , and  $I_3$  are the reverse saturation currents of three diodes, respectively.  $V_t$  is the thermal voltage symbolized by  $kT/q$ , where  $k$  is the Boltzmann's constant,  $T$  is the absolute temperature, and  $q$  is the electron charge. In addition,  $V_D$  is the voltage drop across the recombination diodes and shunt resistance  $R_{sh}$ , equating with  $IR_s + V$  in Fig. 1(c).

Obviously, (1) is an implicit transcendental equation including three exponent items, which is more complicated than  $I$ - $V$  equation of one-diode model in Fig. 1(a) including only one exponent item. It is noted that one diode in circuit topology has a correspondence with one exponent item in  $I$ - $V$  equation. Up to date, transcendental equation including single exponent item could be solved analytically [23]. However, transcendental equation including more than one exponent item is still not able to be solved analytically. This is the reason why we still have difficulty in deriving the terminal  $I$ - $V$  characteristics of both two-diode and three-diode models analytically and implementing them into photovoltaic device and system simulations. In order to overcome the above problem, we are inspired by the effective charge density method [24], [25] applied in thin film transistor compact model to propose the effective-diode method as follows.

In the effective-diode method, we try to make the effect of three diodes equivalent to the effect of single one diode,

which is shown in Fig. 1(c). According to foreign equivalent law, the current going through the effective diode  $D_{eff}$  should be equated with the summary of the recombination currents going through three diodes  $D_1$ - $D_3$ , that is

$$I_{eff} \left( e^{\frac{V_D}{n_{eff} V_t}} - 1 \right) = I_1 \left( e^{\frac{V_D}{n_1 V_t}} - 1 \right) + I_2 \left( e^{\frac{V_D}{n_2 V_t}} - 1 \right) + I_3 \left( e^{\frac{V_D}{n_3 V_t}} - 1 \right). \quad (2)$$

Here  $n_{eff}$  is the effective ideality factor of  $D_{eff}$  representing the divergence from the ideal diode, and  $I_{eff}$  is the effective reverse saturation current of  $D_{eff}$ . We can observe that the constant item of the left-hand side (LHS) formula in (2) should be equal with that of the right-hand side (RHS) formula in (2), yielding

$$I_{eff} = I_1 + I_2 + I_3. \quad (3)$$

Furthermore, to determine  $n_{eff}$  from (2)

$$n_{eff} = \frac{V_D}{V_t \cdot \ln \left( \frac{V_D}{I_{eff} \left( e^{\frac{V_D}{n_1 V_t}} - 1 \right) + I_2 \left( e^{\frac{V_D}{n_2 V_t}} - 1 \right) + I_3 \left( e^{\frac{V_D}{n_3 V_t}} - 1 \right)} \right)}. \quad (4)$$

We have to acquire the results of  $V_D$  from (1) by using the explicit calculation scheme.

In fact, this scheme [12] is the calculation method of deriving the coarse  $V_D$  solution and then correcting it. First, we simplify (1), in the special case of  $n_1 = n_2 = n_3 = n$ , as

$$\frac{V_D - V}{R_s} = I_{ph} - I_1 \left( e^{\frac{V_D}{n V_t}} - 1 \right) - I_2 \left( e^{\frac{V_D}{n V_t}} - 1 \right) - I_3 \left( e^{\frac{V_D}{n V_t}} - 1 \right) - \frac{V_D}{R_{sh}}. \quad (5)$$

Second, we can derive the coarse value of  $V_D$  from (5) and name it as  $V_{D0}$  to be convenient for describing the further analysis. It is noted that  $V_{D0}$  is only valid for (5) or (1) in the special case of  $n_1/n_2/n_3 = 1$ , yielding

$$V_{D0} = R(I_{ph} + I_{eff}) + \frac{RV}{R_s} - nV_t \cdot W_0 \left[ \frac{RI_{eff}}{nV_t} \cdot e^{\frac{R(I_{ph} + I_{eff})}{nV_t} + \frac{R}{R_s} \cdot \frac{V}{nV_t}} \right] \quad (6)$$

where  $R = R_s // R_{sh}$ . In addition, the Lambert  $W$  function has been widely applied into building semiconductor device compact model [14], [24], [25], and  $W_0$  is the Lambert  $W$  function's principal branch [26] as a typical solution to equation  $W_0(x)e^{W_0(x)} = x$ . Subsequently, we substitute  $V_{D0}$  into (5) to obtain the coarse terminal voltage  $V$  labeled as  $V_0$ . That is

$$V_0 = R_s I_1 \left( e^{\frac{V_{D0}}{n_1 V_t}} - 1 \right) + R_s I_2 \left( e^{\frac{V_{D0}}{n_2 V_t}} - 1 \right) + R_s I_3 \left( e^{\frac{V_{D0}}{n_3 V_t}} - 1 \right) + \frac{R_s}{R} \cdot V_{D0} - R_s I_{ph}. \quad (7)$$

Furthermore, we substitute  $V_{D0}$  in (6) for  $V_D$  in three exponent items of (5), substitute  $V_0$  in (7) for  $V$  in (5), and retain variable  $V_D$  in the nonexponent item of (5). Then, we obtain  $V_D$  as

$$V_D = RI_{ph} + \frac{RV_0}{R_{sh}} - RI_1 \left( e^{\frac{V_{D0}}{n_1 V_t}} - 1 \right) - RI_2 \left( e^{\frac{V_{D0}}{n_2 V_t}} - 1 \right) - RI_3 \left( e^{\frac{V_{D0}}{n_3 V_t}} - 1 \right) + \omega. \quad (8)$$

Third, considering that the accuracy of  $V_D$  directly determines the accuracy of  $n_{eff}$  in (4) and the validity of the

effective-diode method, we furthermore improve the accuracy of  $V_D$  by using the third-order Taylor expansion correction  $\omega$  symbolised by  $\omega = -(y/y')(1 + (yy'')/(2y'^2) + (3y^2y''^2 - y^2y'y^{(3)})/(6y'^4))$  in (8). Here,  $y = I_1(e^{V_D/(n_1V_t)} - 1) + I_2(e^{V_D/(n_2V_t)} - 1) + I_3(e^{V_D/(n_3V_t)} - 1) + (V_D/R) - (V/R_s) - I_{ph}$ . In addition,  $y'$ ,  $y''$ , and  $y^{(3)}$  are the first, second, and third derivatives of  $y$  versus  $V_D$ , respectively. Of course, as a kind of high-order corrections [12], [14], [23], [24], three-order Taylor expansion correction [12] is more accurate than two-order Schroder series correction [14], [23], [24], at the cost of efficiency. Then we substitute (8) into (4) to obtain the effective ideality factor  $n_{eff}$ . Finally, after determining the reverse saturation current  $I_{eff}$  in (3) and the effective ideality factor  $n_{eff}$  in (4), we can complete the equivalent transformation shown in Fig. 1(d).

In Fig. 2, the above proposed effective-diode method is verified and proven that it could be used to simplify three-diode model into one-diode model for the different diodes  $D_1$ – $D_3$ . In Fig. 2(a), the diode current  $I_{D3}$  is dominant in the summary of three-diode currents because of  $n_3 < n_2 < n_1$  and  $I_3 > I_2 > I_1$ . In this case, three-diode model degenerates into one-diode-like model actually. In Fig. 2(b), because both  $I_{D2}$  and  $I_{D3}$  take the leading role in  $I_{D1} + I_{D2} + I_{D3}$ , three-diode model degenerates into two-diode-like model. In Fig. 2(c), there is not any one diode current dominating  $I_{D1} + I_{D2} + I_{D3}$ , so that it is the real three-diode model in this case. The figures inset in Fig. 2 show good agreements between  $I_{Deff}$  and  $I_{D1} + I_{D2} + I_{D3}$ , and errors are less than  $10^{-13}$  A. In fact, we can transform multiple-diode model into the effective one-diode model in the above proposed effective-diode method, which is convenient for us to solve  $I$ – $V$  characteristics and four key factors analytically.

### III. ANALYTICAL SOLUTION TO THREE-DIODE MODEL

By using our effective-diode method, we can substitute (2) and equation “ $V_D = IR_s + V$ ” into (1) and obtain the simplified terminal current–voltage equation of three-diode model in Fig. 1(c), yielding

$$I = I_{ph} - I_{eff} \left( e^{\frac{IR_s + V}{n_{eff}V_t}} - 1 \right) - \frac{IR_s + V}{R_{sh}}. \quad (9)$$

Because only one exponent item is included in (9), we can derive the analytical expression of  $I$  as

$$I = \frac{n_{eff}V_t}{R_s} \cdot \left[ z - \frac{V}{n_{eff}V_t} - W_0 \left( \frac{RI_{eff}}{n_{eff}V_t} \cdot e^z \right) \right] \quad (10)$$

where  $z = (R(I_{ph} + I_{eff})) / (n_{eff}V_t) + (1 - (R/R_{sh})) \cdot V / (n_{eff}V_t)$  and  $R = R_s // R_{sh}$ .

Based on (10), we can derive short-circuit current  $I_{sc}$  and open-circuit voltage  $V_{oc}$  analytically. In the case of short-circuit, we substitute  $V = 0$  V into (10) to obtain  $I_{sc}$  as

$$I_{sc} = \frac{n_{eff}V_t}{R_s} \cdot \left[ \frac{RI_{ph} + RI_{eff}}{n_{eff}V_t} - W_0 \left( \frac{RI_{eff}}{n_{eff}V_t} \cdot e^{\frac{RI_{ph} + RI_{eff}}{n_{eff}V_t}} \right) \right]. \quad (11)$$

In the case of open-circuit, we substitute  $I = 0$  A into (10) to obtain  $V_{oc}$  as

$$V_{oc} = R(I_{ph} + I_{eff}) - n_{eff}V_t \cdot W_0 \left( \frac{RI_{eff}}{n_{eff}V_t} \cdot e^{\frac{RI_{ph} + RI_{eff}}{n_{eff}V_t}} \right). \quad (12)$$

According to the analytical expression (10) of  $I$ , we can obtain the power function  $P = I \cdot V$  as

$$P = \frac{n_{eff}V_t}{R_s} \cdot \left[ z \cdot V - \frac{V^2}{n_{eff}V_t} - V \cdot W_0 \left( \frac{RI_{eff}}{n_{eff}V_t} \cdot e^z \right) \right]. \quad (13)$$

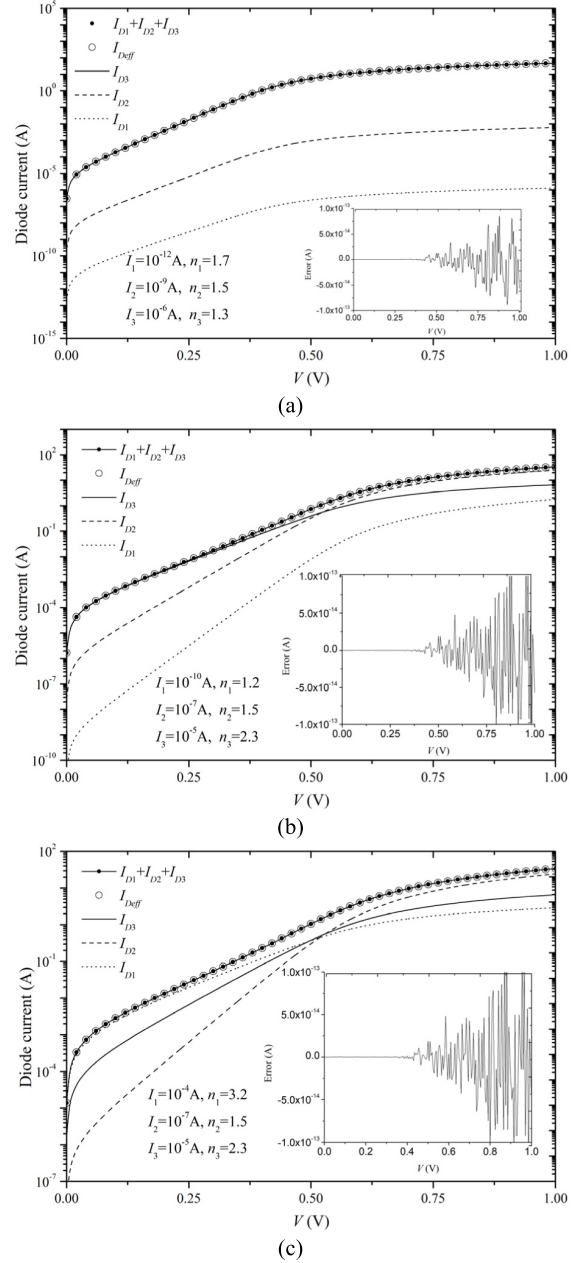


Fig. 2. Effective-diode current  $I_{Deff}$  and three diode currents  $I_{D1}$ ,  $I_{D2}$ , and  $I_{D3}$  in Fig. 1(c). (a) One-diode-like model. (b) Two-diode-like model. (c) Real three-diode model.

To find out the maximum power point ( $V_m$ ,  $P_m$ ), we make derivative  $(dP)/(dV)$  of  $P$  versus  $V$  equal to zero, yielding

$$\frac{R(I_{ph} + I_{eff})}{R_s} - \frac{2RV_m}{R_{sh}R_s} - \frac{n_{eff}V_t}{R_s} \cdot W_0 \left( \frac{RI_{eff}}{n_{eff}V_t} \cdot e^{z_m} \right) - \frac{R_{sh} - R}{R_{sh}R_s} \cdot \frac{V_m \cdot W_0 \left( \frac{RI_{eff}}{n_{eff}V_t} \cdot e^{z_m} \right)}{1 + W_0 \left( \frac{RI_{eff}}{n_{eff}V_t} \cdot e^{z_m} \right)} = 0. \quad (14)$$

Obviously, (14) is too complicated to solve the analytical solution of  $V_m$  directly, where  $z_m = (R(I_{ph} + I_{eff})) / (n_{eff}V_t) + (1 - (R/R_{sh})) \cdot (V_m / n_{eff}V_t)$ . Here we have to derive the coarse solution and then correct it. From the circuit topology aspect, we can observe that three-diode model actually is nonlinear circuit. From the mathematical derivation aspect, (14) is also



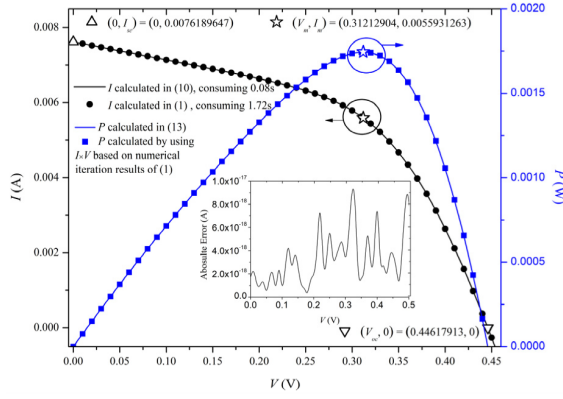


Fig. 3.  $I$  versus  $V$  and  $P$  versus  $V$  in three-diode model.

nonlinear equation. Fortunately, Lambert  $W$  function  $W_0(x)$  has progressive expansion equation retaining the first two items, i.e.,  $W_0(x) \approx \ln x - \ln \ln x$ . Substituting it into (14), we can observe that (14) can degenerate into linear-like equation. Therefore, there is simplified linear circuit, i.e., resistance circuit, corresponding to nonlinear circuit in Fig. 1(c). Here by using maximum power law of linear circuit,  $V_{oc}$ , and  $I_{sc}$ , we derive the coarse maximum power point ( $V_{m0}$ ,  $P_{m0}$ ) as follows. Of course, it is only suitable for linear circuit as the approximate solution to the maximum power point ( $V_m$ ,  $P_m$ ) of nonlinear circuit in Fig. 1(c).

First, we can obtain the output resistance of circuit Fig. 1(c) as  $R_{out} = V_{oc}/I_{sc}$ . Second, according to maximum power law, we can determine that the maximum power is acquired in the case of  $R_L = R_{out}$  in Fig. 1(c). At this time, we obtain the implicit equation about  $V_D$  as

$$I_{ph} = I_{eff} \left( e^{\frac{V_D}{n_{eff} V_t}} - 1 \right) + \frac{V_D}{R_{sh}} + \frac{V_D}{R_s + R_L}. \quad (15)$$

Then, we derive  $V_D$  as

$$V_D = R(I_{ph} + I_{eff}) - n_{eff} V_t \cdot W_0 \left[ \frac{R_{sh}(R_s + R_L)I_{eff}}{n_{eff} V_t (R_{sh} + R_s + R_L)} \cdot e^{\frac{R_{sh}(R_s + R_L)(I_{ph} + I_{eff})}{n_{eff} V_t (R_{sh} + R_s + R_L)}} \right]. \quad (16)$$

Third, we determine  $V_{m0}$  as

$$V_{m0} = \frac{R_L}{R_s + R_L} \cdot V_D. \quad (17)$$

Subsequently, we obtain  $P_{m0}$  as  $P_{m0} = (V_{m0}^2/R_L)$ . It is noted that ( $V_{m0}$ ,  $P_{m0}$ ) as the coarse value is not accurate enough for the three-diode circuit model in Fig. 1(c). To improve the accuracy of the maximum power point ( $V_m$ ,  $P_m$ ) and make it valid for the nonlinear three-diode circuit model, we also use the third-order Taylor expansion correction  $\omega$  [12] symbolized by

$$\omega = -\frac{y}{y'} \left( 1 + \frac{y y''}{2 y'^2} + \frac{3 y^2 y''^2 - y^2 y' y'''}{6 y'^4} \right). \quad (18)$$

Here  $y$  is acquired from (15) as

$$y = \frac{R(I_{ph} + I_{eff})}{R_s} - \frac{2 R V_m}{R_{sh} R_s} - \frac{n_{eff} V_t}{R_s} \cdot W_0(\eta) - \frac{R_{sh} - R}{R_{sh} R_s} \cdot \frac{V_m \cdot W_0(\eta)}{1 + W_0(\eta)} \quad (19)$$

where  $\eta = (R I_{eff}) / (n_{eff} V_t) \cdot e^{z_m}$ . In addition,

$$y' = -\frac{2 R}{R_{sh} R_s} - \frac{2 n_{eff} V_t}{R_s} \cdot W_0'(\eta) - \frac{n_{eff} V_t}{R_s} \cdot V \cdot W_0''(\eta) \quad (20)$$

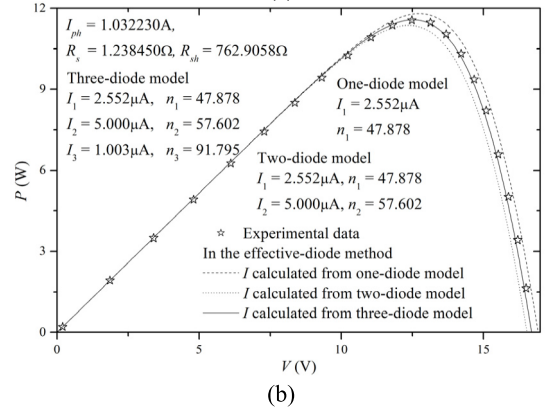
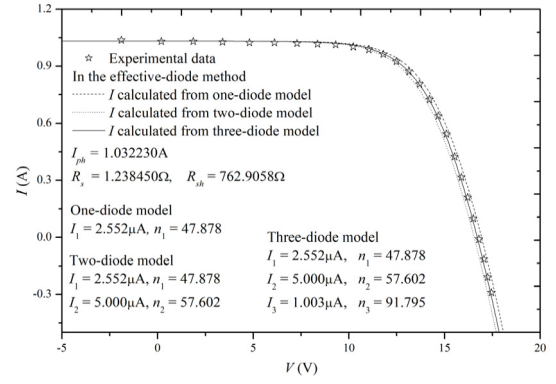


Fig. 4. Experimental data [27] measured from photo watt-PWP 201 PV module at 1000 W/m<sup>2</sup> irradiance and  $T = 45^\circ\text{C}$ , and simulation results in effective-diode method for (a)  $I$  versus  $V$  and (b)  $P$  versus  $V$ .

$$y'' = -\frac{3 n_{eff} V_t}{R_s} \cdot W_0''(\eta) - \frac{n_{eff} V_t}{R_s} \cdot V \cdot W_0'''(\eta) \quad (21)$$

$$y''' = -\frac{4 n_{eff} V_t}{R_s} \cdot W_0'''(\eta) - \frac{n_{eff} V_t}{R_s} \cdot V \cdot W_0^{(4)}(\eta). \quad (22)$$

Here  $W_0'(\eta) = (1 - R/(R_{sh})) \cdot 1/(n_{eff} V_t) \cdot (W_0(\eta))/(1 + W_0(\eta))$ ,  $W_0''(\eta) = (1 - R/(R_{sh})) \cdot 1/(n_{eff} V_t) \cdot (W_0'(\eta))/([1 + W_0(\eta)]^2)$ ,  $W_0'''(\eta) = (1 - R/(R_{sh})) \cdot 1/(n_{eff} V_t) \cdot (W_0''(\eta)[1 + W_0(\eta)]^2 - 2[1 + W_0(\eta)]W_0'^2(\eta))/([1 + W_0(\eta)]^4)$ ,  $W_0^{(4)}(\eta) = (1 - R/(R_{sh})) \cdot 1/(n_{eff} V_t) \cdot \{(W_0'''(\eta)[1 + W_0(\eta)]^4 - 2[1 + W_0(\eta)]W_0''(\eta)W_0'(\eta))/([1 + W_0(\eta)]^4) - (4W_0'(\eta)W_0''(\eta)[1 + W_0(\eta)]^3 - 3[1 + W_0(\eta)]^2W_0'^2(\eta) \cdot 2W_0'^2(\eta))/([1 + W_0(\eta)]^6)\}$ . Moreover,  $V_m$  is expressed as

$$V_m = V_{m0} + \omega. \quad (23)$$

By substituting (23) into (10), we can obtain  $I_m$  as

$$I_m = \frac{n_{eff} V_t}{R_s} \cdot \left[ z_m - \frac{V_m}{n_{eff} V_t} - W_0 \left( \frac{R I_{eff}}{n_{eff} V_t} \cdot e^{z_m} \right) \right]. \quad (24)$$

Finally,  $P_m$  and FF are demonstrated as

$$P_m = I_m V_m \quad (25)$$

$$\text{FF} = P_m / I_{sc} V_{oc}. \quad (26)$$

Here we use these numerical iteration results to verify our analytical solutions of three-diode model based on our effective-diode method, as shown in Fig. 3. Good agreements show that our analytical solution is both accurate and efficient. The maximum absolute error of  $I$ - $V$  curves between effective-diode-based solutions and numerical iteration results is less than  $10^{-17}$  A. Computation efficiency is improved by two orders of magnitude.

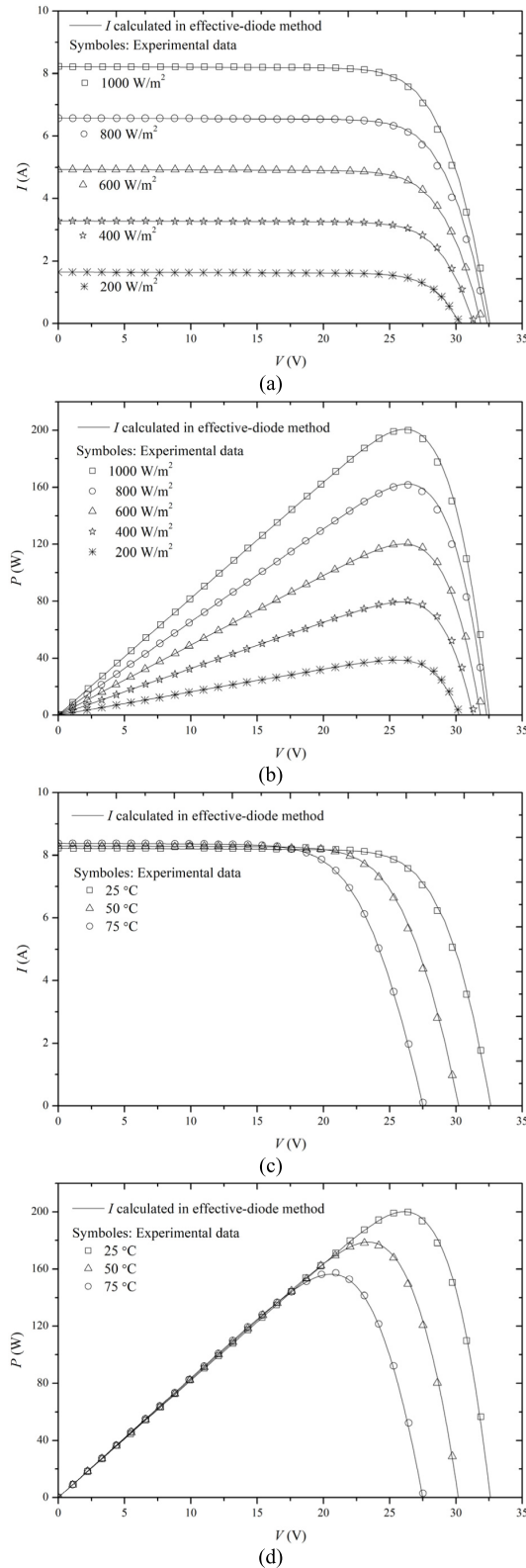


Fig. 5. Experimental data [28] measured from KC200GT PV module on different irradiances and temperatures for (a) and (c)  $I$  versus  $V$  and (b) and (d)  $P$  versus  $V$ .

#### IV. EXPERIMENTAL VERIFICATIONS

In this section, the proposed analytical solution to three-diode lumped-parameter model of industrial solar cells is validated by experimental data measured from industrial

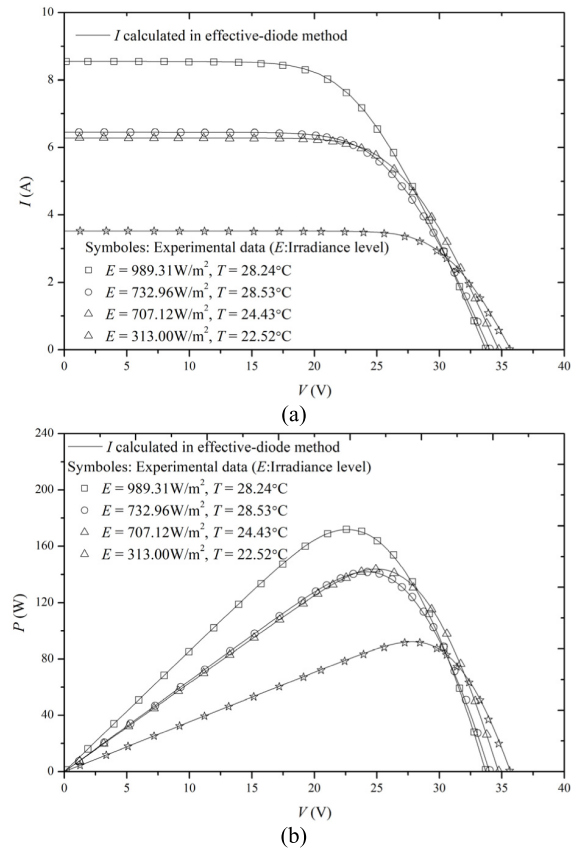


Fig. 6. Experimental data [29] measured from IFRI250-60 module on different irradiances and temperatures for (a)  $I$  versus  $V$  and (b)  $P$  versus  $V$ .

multicrystalline PV modules, including Photo Watt-PWP 201 [27], KC200GT [28], and IFRI250-60 [29]. The simulation results and experimental data are reported and shown in the following figures. Here fitting parameters in simulations could be defined by using the common routine of parameter extraction, such as intelligent computational algorithms [30]. Obviously, good agreements validate the practicability and accuracy of the proposed effective-diode-method-based analytical solution to solar cells' lumped-parameter model.

First, photo Watt-PWP 201 PV module [27] comprises a series connection of 36 polycrystalline silicon cells. The  $I$ - $V$  and  $P$ - $V$  characteristics are measured and calculated at an irradiance level of  $1000 \text{ W/m}^2$  and a temperature of  $45^\circ\text{C}$ , as shown in Fig. 4. In addition, simulation results of one-, two-, and three-diode models are shown in Fig. 4 simultaneously. It is as well-known that, because large amount of defects and grain sites existing in polycrystalline silicon cells lead to large leakage current, the contribution of recombination current  $I_{D3}$  resulting from defects and grain sites must be considered in the lumped-parameter model of solar cells. We can observe that three-diode model processes higher accuracy than both one- and two-diode models for simulating  $I$ - $V$  and  $P$ - $V$  curves of industrial multicrystalline PV modules. Here root mean square errors of one-, two-, and three-diode models are 0.0542, 0.0374, and 0.000103, respectively. This point is also consistent with the results shown in Fig. 4.

Second, the experimental data measured from KC200GT [28] at three different temperatures are also used to confirm the accuracy of the proposed effective-diode method solution to three-diode model. On the one hand,

as shown in Fig. 5(a) and (b), irradiance level has little effects on the open-circuit voltage  $V_{oc}$ , but it has important effects on the short-circuit current  $I_{sc}$ . On the other hand, as shown in Fig. 5(c) and (d), temperature plays an important role in determining the open-circuit voltage  $V_{oc}$  instead of the short-circuit current  $I_{sc}$ .

Third, we use the experimental data measured from IFRI250-60 [29] to verify the further practicability of the proposed effective-diode method solution to three-diode model. Fig. 6 shows that simulation results match well with experimental data at arbitrary irradiance levels and temperatures.

## V. CONCLUSION

In this article, we proposed the effective-diode method to simplify three-diode lumped-parameter model and solve  $I$ - $V$  characteristics of industrial solar cells analytically. Based on effective-diode-solution, we achieved the important four feature parameters, i.e., short-circuit current, open-circuit voltage, maximum power point, and FF, by deriving the coarse solution analytically and then correcting it. Finally, we used numerical iteration method to validate the accuracy and efficiency of our effective-diode method and then adopted experimental data of industrial solar cells to verify the practicability. As a result, the effective-diode method can be used to complete simulation and analysis for  $I$ - $V$  characteristics of industrial solar cells and make it possible for us to implement the three-diode model into solar cells' simulators.

## REFERENCES

- [1] L. H. I. Lim, Z. Ye, J. Ye, D. Z. Yang, and H. Du, "A linear identification of diode models from single  $IV$  characteristics of PV panels," *IEEE Trans. Ind. Electron.*, vol. 62, no. 7, pp. 4181–4193, Jul. 2015, doi: [10.1109/TIE.2015.2390193](#).
- [2] H.-L. Tsai, "Insolation-oriented model of photovoltaic module using MATLAB/simulink," *Sol. Energy*, vol. 84, no. 7, pp. 1318–1326, Jul. 2010, doi: [10.1016/j.solener.2010.04.012](#).
- [3] E. Saloux, A. Teyssedou, and M. Sorin, "Explicit model of photovoltaic panels to determine voltages and currents at the maximum power point," *Sol. Energy*, vol. 85, no. 5, pp. 713–722, May 2011, doi: [10.1016/j.solener.2010.12.022](#).
- [4] K. Ishaque, Z. Salam, and H. Taheri, "Simple, fast and accurate two-diode model for photovoltaic modules," *Sol. Energy Mater. Sol. Cells*, vol. 95, no. 2, pp. 586–594, Feb. 2011, doi: [10.1016/j.solmat.2010.09.023](#).
- [5] H. Patel and V. Agarwal, "MATLAB-based modeling to study the effects of partial shading on PV array characteristics," *IEEE Trans. Energy Convers.*, vol. 23, no. 1, pp. 302–310, Mar. 2008, doi: [10.1109/TEC.2007.914308](#).
- [6] K. Nishioka, N. Sakitani, Y. Uraoka, and T. Fuyuki, "Analysis of multicrystalline silicon solar cells by modified 3-diode equivalent circuit model taking leakage current through periphery into consideration," *Sol. Energy Mater. Sol. Cells*, vol. 91, no. 13, pp. 1222–1227, Aug. 2007, doi: [10.1016/j.solmat.2007.04.009](#).
- [7] A. Ortiz-Conde, D. Lugo-Muñoz, and F. J. García-Sánchez, "An explicit multiexponential model as an alternative to traditional solar cell models with series and shunt resistances," *IEEE J. Photovolt.*, vol. 2, no. 3, pp. 261–268, Jul. 2012, doi: [10.1109/JPHOTOV.2012.2190265](#).
- [8] V. Khanna, B. K. Das, D. Bisht, Vandana, and P. K. Singh, "A three diode model for industrial solar cells and estimation of solar cell parameters using PSO algorithm," *Renew. Energy*, vol. 2, no. 3, pp. 261–268, Jul. 2012, doi: [10.1016/j.renene.2014.12.072](#).
- [9] F. García-Sánchez *et al.*, "Modelling solar cell S-shaped  $I$ - $V$  characteristics with DC lumped-parameter equivalent circuits a review," *Facta Universitatis, Electron. Energetics*, vol. 30, no. 3, pp. 327–350, Sep. 2017, doi: [10.2298/FUEE1703327G](#).
- [10] F. A. De Castro, J. Heier, F. Nüesch, and R. Hany, "Origin of the kink in current-density versus voltage curves and efficiency enhancement of polymer- $C_{60}$  heterojunction solar cells," *IEEE J. Sel. Topics Quantum Electron.*, vol. 16, no. 6, pp. 1690–1699, Nov./Dec. 2010, doi: [10.1109/JSTQE.2010.2040807](#).
- [11] R. V. K. Chavali, J. V. Li, C. Battaglia, S. De Wolf, J. L. Gray, and M. A. Alam, "A generalized theory explains the anomalous suns- $V_{oc}$  response of Si heterojunction solar cells," *IEEE J. Photovolt.*, vol. 7, no. 1, pp. 169–176, Nov./Dec. 2017, doi: [10.1109/JPHOTOV.2016.2621346](#).
- [12] F. Yu, G. Huang, W. Lin, and C. Xu, "Lumped-parameter equivalent circuit model for S-shaped current-voltage characteristics of organic solar cells," *IEEE Trans. Electron Devices*, vol. 66, no. 1, pp. 670–677, Jan. 2019, doi: [10.1109/TED.2018.2878465](#).
- [13] A. Jain and A. Kapoor, "A new approach to study organic solar cell using Lambert W-function," *Sol. Energy Mater. Sol. Cells*, vol. 86, no. 2, pp. 197–205, Mar. 2005, doi: [10.1016/j.solmat.2004.07.004](#).
- [14] F. Yu, G. Huang, W. Lin, and C. Xu, "An analysis for S-shaped  $I$ - $V$  characteristics of organic solar cells using lumped-parameter equivalent circuit model," *Sol. Energy*, vol. 177, pp. 229–240, Jan. 2019, doi: [10.1016/j.solener.2018.11.011](#).
- [15] R. Abbassi, A. Abbassi, M. Jemli, and S. Chebbi, "Identification of unknown parameters of solar cell models: A comprehensive overview of available approaches," *Renew. Sustain. Energy Rev.*, vol. 90, pp. 453–474, Jul. 2018, doi: [10.1016/j.rser.2018.03.011](#).
- [16] D. S. H. Chan, J. R. Phillips, and J. C. H. Phang, "A comparative study of extraction methods for solar cell model parameters," *Solid-State Electron.*, vol. 29, no. 3, pp. 329–337, Mar. 1986, doi: [10.1016/0038-1101\(86\)90212-1](#).
- [17] C. Zhang, J. Zhang, Y. Hao, Z. Lin, and C. Zhu, "A simple and efficient solar cell parameter extraction method from a single current-voltage curve," *J. Appl. Phys.*, vol. 110, no. 6, Sep. 2011, Art. no. 064504, doi: [10.1063/1.3632971](#).
- [18] S. P. Mallick, D. P. Dash, S. Mallik, R. Roshan, and S. Mahata, "An empirical approach towards photovoltaic parameter extraction and optimization," *Sol. Energy*, vol. 153, pp. 360–365, Sep. 2017, doi: [10.1016/j.solener.2017.05.076](#).
- [19] N. Boutana, A. Mellit, V. Lughi, and A. M. Pavan, "Assessment of implicit and explicit models for different photovoltaic modules technologies," *Energy*, vol. 122, pp. 128–143, Mar. 2017, doi: [10.1016/j.energy.2017.01.073](#).
- [20] A. Laudani, F. R. Fulginei, F. De Castro, and A. Salvini, "Irradiance intensity dependence of the lumped parameters of the three-diodes model for organic solar cells," *Sol. Energy*, vol. 163, pp. 526–536, Mar. 2018, doi: [10.1016/j.solener.2018.02.032](#).
- [21] F. De Castro, A. Laudani, F. R. Fulginei, and A. Salvini, "An in-depth analysis of the modelling of organic solar cells using multiple-diode circuits," *Sol. Energy*, vol. 135, pp. 590–597, Oct. 2016, doi: [10.1016/j.solener.2016.06.033](#).
- [22] W. Shockley, "The theory of  $p$ - $n$  junctions in semiconductors and  $p$ - $n$  junction transistors," *Bell Syst. Tech. J.*, vol. 28, no. 3, pp. 435–489, Jul. 1949, doi: [10.1002/j.1538-7305.1949.tb03645.x](#).
- [23] F. Yu, W. Deng, J. Huang, X. Ma, and S. Chen, "An explicit physics-based  $I$ - $V$  model for surrounding-gate polysilicon transistors," *IEEE Trans. Electron Devices*, vol. 63, no. 3, pp. 1059–1065, Mar. 2016, doi: [10.1109/TED.2015.2512851](#).
- [24] W. Deng, J. Huang, X. Ma, and T. Ning, "An explicit surface-potential-based model for amorphous IGZO thin-film transistors including both tail and deep states," *IEEE Electron Device Lett.*, vol. 35, no. 1, pp. 78–80, Jan. 2014, doi: [10.1109/LED.2013.2289877](#).
- [25] F. Yu, W. Deng, J. Huang, X. Ma, and J. J. Liou, "A physics-based compact model for symmetrical double-gate polysilicon thin-film transistors," *IEEE Trans. Electron Devices*, vol. 64, no. 5, pp. 2221–2227, May 2017, doi: [10.1109/TED.2017.2679340](#).
- [26] R. M. Corless, G. H. Gonnet, D. E. G. Hare, D. J. Jeffrey, and D. E. Knuth, "On Lambert's W function," *Adv. Comput. Math.*, vol. 5, pp. 329–359, May 1996, doi: [10.1007%2FBF02124750](#).
- [27] T. Easwarakhanthan, J. Bottin, I. Bouhouch, and C. Boutrix, "Nonlinear minimization algorithm for determining the solar cell parameters with microcomputers," *Int. J. Sol. Energy*, vol. 4, no. 1, pp. 1–12, Jan. 1986, doi: [10.1080/01425918608909835](#).
- [28] *Kc200gt, High Efficiency Multicrystal Photovoltaic Module*. [Online]. Available: <https://www.kycerasolar.com/dealers/product-center/archives/spec-sheets/KC200GT.pdf>
- [29] *IFRI-250-60 Poly-Crystalline PV Module*. [Online]. Available: [https://akafi.net/storage/upload/1179625\\_1408966265.pdf](https://akafi.net/storage/upload/1179625_1408966265.pdf)
- [30] T. Wei, F. Yu, G. Huang, and C. Xu, "A particle-swarm-optimization-based parameter extraction routine for three-diode lumped parameter model of organic solar cells," *IEEE Electron Device Lett.*, vol. 40, no. 9, pp. 1511–1514, Sep. 2019.